Published in final edited form as:

Cell Rep. 2018 May 29; 23(9): 2678–2689. doi:10.1016/j.celrep.2018.04.107.

NMDA Receptor Activation Underlies the Loss of Spinal Dorsal Horn Neurons and the Transition to Persistent Pain after Peripheral Nerve Injury

Perrine Inquimbert[1,2,10], **Martin Moll**[3,4,10], **Alban Latremoliere**[2,5], **Chi-Kun Tong**[3], **John Whang**[3], **Gregory F. Sheehan**[3], **Brendan M. Smith**[3], **Erica Korb**[6], **Maria C.P. Athié**[7], **Olusegun Babaniyi**[2], **Nader Ghasemlou**[2], **Yuchio Yanagawa**[8], **C. David Allis**[6], **Patrick R. Hof**[9], and **Joachim Scholz**[3,11,*]

[1]Centre National de la Recherche Scientifique, UPR 3212, Institut des Neurosciences Cellulaires et Intégratives and Université de Strasbourg, 67084 Strasbourg, France

[2]F.M. Kirby Neurobiology Center, Boston Children's Hospital and Department of Neurobiology, Harvard Medical School, Boston, MA 02115, USA

[3]Departments of Anesthesiology and Pharmacology, Columbia University Medical Center, New York, NY 10032, USA

[4]Institute of Pharmacology, Heidelberg University, 69120 Heidelberg, Germany

[5]Department of Neurology and Neurosurgery, Johns Hopkins University School of Medicine, Baltimore, MD 21287, USA

[6]Laboratory of Chromatin Biology and Epigenetics, Rockefeller University, New York, NY 10065, USA

[7]Department of Structural and Functional Biology, State University of Campinas, Campinas, SP 13083-865, Brazil

[8]Department of Genetic and Behavioral Neuroscience, Gunma University Graduate School of Medicine, Maebashi, Gunma 371-8511, Japan

[9]Fishberg Department of Neuroscience and Friedman Brain Institute, Icahn School of Medicine at Mount Sinai, New York, NY 10029, USA

[10]These authors contributed equally

[*]Correspondence: scholz.joachim@gmail.com.

AUTHOR CONTRIBUTIONS

P.I., M.M., and J.S. designed the experiments. P.I., M.M., A.L., C.-K.T., J W., G.F.S., B.M.S., E.K., M.C.P.A., O.B., and N.G. collected and analyzed the results.Y.Y., C.D.A., and P.R.H. contributed to the study design and the interpretation of findings. P.I., M.M., and J.S. wrote the manuscript.

SUPPLEMENTAL INFORMATION

Supplemental Information includes Supplemental Experimental Procedures, five figures, and two tables and can be found with this article online at https://doi.org/10.1016/j.celrep.2018.04.107.

DECLARATION OF INTERESTS

J.S. is now an employee of Biogen. This work was completed before he joined the company. The company did not have a role in the design, conduct, analysis, interpretation, or funding of the research. All other authors declare no competing interests.

[11]Lead Contact

SUMMARY

Peripheral nerve lesions provoke apoptosis in the dorsal horn of the spinal cord. The cause of cell death, the involvement of neurons, and the relevance for the processing of somatosensory information are controversial. Here, we demonstrate in a mouse model of sciatic nerve injury that glutamate-induced neurodegeneration and loss of γ-aminobutyric acid (GABA)ergic interneurons in the superficial dorsal horn promote the transition from acute to chronic neuropathic pain. Conditional deletion of *Grin1*, the essential subunit of *N*-methyl-D-aspartate-type glutamate receptors (NMDARs), protects dorsal horn neurons from excitotoxicity and preserves GABAergic inhibition. Mice deficient in functional NMDARs exhibit normal nociceptive responses and acute pain after nerve injury, but this initial increase in pain sensitivity is reversible. Eliminating NMDARs fully prevents persistent pain-like behavior. Reduced pain in mice lacking proapoptotic *Bax* confirmed the significance of neurodegeneration. We conclude that NMDAR-mediated neuron death contributes to the development of chronic neuropathic pain.

In Brief

Dorsal horn neurons process somatosensory information, including pain. Inquimbert et al. utilized spatially restricted *Grin1* knockout to show that NMDA-receptor-mediated excitatory input causes the degeneration of some dorsal horn neurons after nerve injury. Irreversible loss of GABAergic interneurons leads to a deficit in inhibition that promotes persistent pain hypersensitivity.

Graphical Abstract

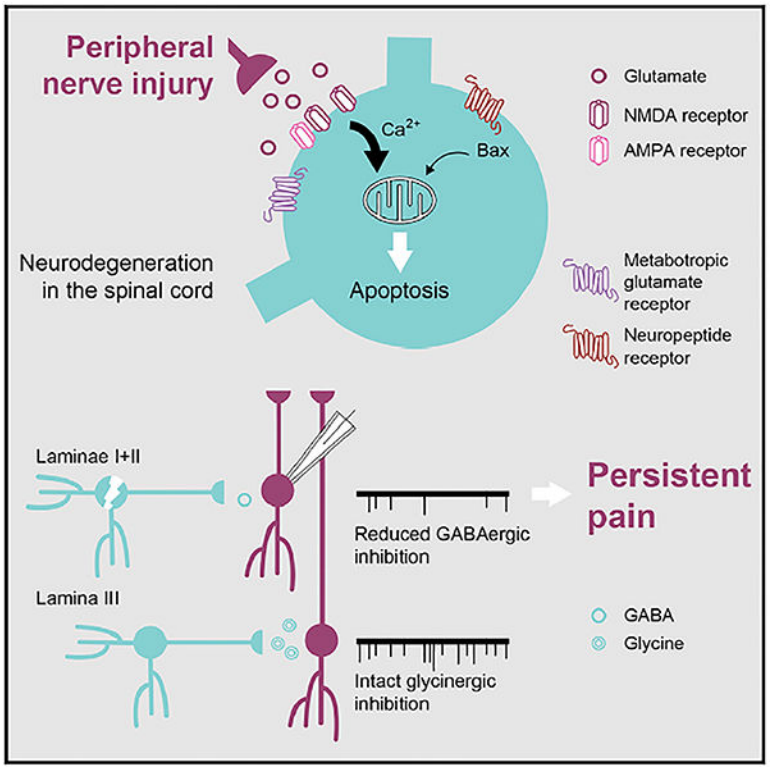

INTRODUCTION

A key characteristic of pain caused by a lesion or disease of the nervous system (neuropathic pain) is its persistence (Colloca et al., 2017). Preclinical studies have revealed that multiple molecular changes in primary sensory neurons, plasticity of central nociceptive connections, and neuroinflammation collectively contribute to the development of neuropathic pain (von Hehn et al., 2012). Many of these investigations focus on the onset of pain during the first one or two weeks following nerve injury. It is increasingly clear though that the involvement of individual pain mechanisms changes with time. Microglia, for example, promote the onset of neuropathic pain through cytokine and growth factor release in the spinal cord (Peng et al., 2016). In contrast, astrocytes respond to nerve injury with a delay of several days or weeks and appear to support the maintenance of pain rather than its initial development (Ji et al., 2014; Scholz and Woolf, 2007). Although insight into the short- and long-term changes of the nociceptive system after nerve injury has improved, the mechanisms driving the transition from acute to chronic pain remain to be resolved.

One process potentially linked to the emergence of persistent pain is the apoptosis of dorsal horn neurons. A loss of dorsal horn neurons after nerve injury has been found in independent studies (Yowtak et al., 2013; Scholz et al., 2005). Conflicting reports may be explained by inadequate statistical power because they relied on the analysis of a single section per spinal cord and an unconventional stereological design that has not been validated (Polgár et al., 2004, 2005). However, the mechanisms responsible for the induction of apoptosis are unknown and its functional significance has been disputed (Polgár et al., 2005). Clarifying the etiology and relevance of nerve-injury-induced neurodegeneration is essential because neuroprotection may offer a disease-modifying treatment strategy for neuropathic pain.

We have previously shown that afferent input from the injured nerve promotes the apoptosis induction (Scholz et al., 2005). The major transmitter of primary sensory neurons at central nociceptive synapses of the dorsal horn is glutamate. Postsynaptic insertion of α-amino-3-hydroxy-5-methyl-4-isoxazolepropionic acid-type glutamate receptors (AMPARs), voltage-dependent recruitment of *N*-methyl-D-aspartate receptors (NMDARs), and changes in the composition of postsynaptic densities strengthen glutamatergic transmission following a nerve lesion (Kuner, 2010; Latremoliere and Woolf, 2009). Activation of NMDARs is critical for this process of central sensitization because it leads to enhanced Ca^{2+} influx and the engagement of intracellular signaling pathways that amplify the response to nociceptive input. However, excess Ca^{2+} increases may cause neuron death, and extrasynaptic NMDAR activation may suppress survival-promoting genes (Hara and Snyder, 2007; Hardingham et al., 2002). To test whether nerve injury produces an excitotoxic challenge in the spinal cord, we selectively eliminated NMDARs in dorsal horn neurons of adult mice. Unlike pharmacological inhibition, this targeted genetic approach did not interfere with presynaptic glutamatergic transmission or NMDAR activity in supraspinal pathways. We found that the conditional deletion of NMDARs at dorsal horn synapses provided effective neuro-protection and blocked the transition from acute to persistent neuropathic-pain-like behavior without affecting physiological nociception. Mice lacking proapoptotic Bcl2-associated × (Bax) showed a similar reduction of chronic pain after nerve injury, confirming the functional impact of neurodegeneration.

RESULTS

Eliminating Functional NMDARs Abolishes Nerve-Injury-Induced Apoptosis

We examined the induction of apoptosis after spared nerve injury (SNI), a partial sciatic nerve lesion associated with persistent pain hypersensitivity in rodents (Figure 1A; Decosterd and Woolf, 2000). Terminal deoxynucleotidyl transferase dUTP nick end labeling (TUNEL) revealed cell profiles with chromatin changes indicative of apoptosis in the dorsal horn of C57BL/6 mice 7 days after SNI (Figure 1B). Most of these profiles were located in the medial dorsal horn of spinal cord segment L4 (Figure 1C), in a distribution corresponding to the central projections of the lesioned common peroneal and tibial branches of the sciatic nerve (Corder et al., 2010). Apoptosis induction continued for 2 weeks and was limited to the ipsilateral dorsal horn (Figures 1D and 1E).

To test the involvement of NMDAR-mediated glutamatergic transmission, we utilized transgenic mice with a floxed sequence of the *Grin1* gene (Tsien et al., 1996). *Grin1* encodes NMDAR subunit GluN1, which is required for the assembly of functional receptors. Stereotaxic injection of an adeno-associated virus (AAV8) with a plasmid encoding a fusion protein of Cre recombinase and GFP eliminated *Grin1* expression and NMDAR activity in the spinal cord within 2 or 3 weeks (Figures 1F, 1G, and S1A). The loss of NMDAR-mediated transmission was a direct result of transgene recombination and not related to AAV8 infection or GFP expression. NMDA-evoked currents in $Grin1^{flox/flox}$ mice in jected with a GFP-encoding control vector did not differ from those in uninjured C57BL/6 mice or C57BL/6 mice after SNI (Figure 1G). To examine the effect of conditional *Grin1* deletion on apoptosis induction, we first injected $Grin1^{flox/flox}$ mice with AAV8-*GFP-Cre* and waited 3 weeks to ensure complete recombination before performing SNI. Seven days after the nerve lesion, we found that apoptotic profiles in the dorsal horn were markedly reduced compared to mice injected with the control vector AAV8-*GFP* (Figure 1H).

Grin1 Deletion Prevents Neuron Loss

AAV8 infection and *Cre* expression were restricted to dorsal horn neurons (Figures S1B–S1F). To examine the efficacy of neuro-protection provided by NMDAR elimination, we conducted a stereological analysis of neuron survival. Because apoptosis induction was concentrated within the distribution of central terminals of the injured sciatic nerve branches, we counted neurons immunostained for neuronal nuclei protein (NeuN) in the medial half of the dorsal horn. We performed these counts 4 weeks after SNI, assuming that neurodegeneration would be complete at this time. SNI led to a decrease in the number of dorsal horn neurons by 25% (95% confidence interval [CI] 16%–35%; $p < 0.001$) in laminae I+II and 14% (95% confidence interval 4.1%–24%; $p < 0.01$) in laminae III+IV (Figures 2A and 2B). $Grin1^{flox/flox}$ mice in jected with AAV8-*GFP-Cre* were fully protected against the loss of neurons. The number of dorsal horn neurons in these mice after SNI did not differ from that in uninjured C57BL/6 mice. In contrast, neurons in $Grin1^{flox/flox}$ mice injected with the control vector AAV8-*GFP* were reduced by 19% in both laminae I+II (95% CI 4.4%–34%; $p < 0.05$) and laminae III+IV (95% CI2.6%–36%; $p < 0.05$; Figures 2C and 2D).

NMDAR-Mediated Neuron Death Impairs Spinal Inhibition

γ-aminobutyric acid (GABA)ergic and glycinergic inhibition is essential for the processing of nociceptive information (Peirs and Seal, 2016). Pharmacological blockade of inhibitory signal transmission, experimental ablation, or silencing of inhibitory dorsal horn neurons provoke spontaneous pain-like behavior and exaggerated reactions to painful stimuli (Cui et al., 2016; Foster et al., 2015; Petitjean et al., 2015; Duan et al., 2014; Lu et al., 2013). Whether nerve-injury-induced neurodegeneration in the dorsal horn involves inhibitory neurons is controversial (Yowtak et al., 2013; Scholz et al., 2005; Polgár et al., 2003).

To address this issue, we first determined whether SNI caused a decrease in GABAergic neurons. For this purpose, we used mice that express *GFP* under the promotor for *glutamate decarboxylase 1* (*Gad1*), a marker of GABAergic neurons (Figure 3A; Tamamaki et al., 2003). Four weeks after SNI, we found GABAergic neurons in laminae I+II of the L4 spinal cord reduced by 10% (95% CI 0.4%–20%; $p < 0.05$). The number of GABAergic neurons in laminae III+IV did not change (Figure 3B). Lamina III and lower contain the majority of glycinergic dorsal horn neurons. Most of these neurons are also GABAergic, but those that produce glycine only would not be fluorescently labeled in *Gad1-GFP* mice (Zeilhofer et al., 2012). To account for these neurons, we utilized mice that express the yellow fluorescent protein *Venus* under the promoter for *vesicular inhibitory amino acid transporter* (*Viaat*), a marker of both GABAergic and glycinergic neurons (Figure 3C; Wang et al., 2009). Stereological analysis of neurons expressing *Venus* confirmed that the number of inhibitory neurons in laminae III+IV did not decline after SNI (Figure 3D).

Next, we tested whether neuroprotection by *Grin1* deletion maintained the functional integrity of inhibitory neurons. To this end, we analyzed miniature inhibitory postsynaptic currents (mIPSCs) from neurons in lamina II and the border to lamina III in slices of the L4 spinal cord of C57BL/6 mice. Following SNI, the frequency of mIPSCs decreased by 69% ($p < 0.001$). The current amplitude did not change, indicating a presynaptic cause of the inhibitory deficit (Figure 3E). Patch-clamp recordings from the spinal cord of $Grin1^{flox/flox}$ mice with intact NMDARs showed a similar low frequency of total mIPSCs after SNI. However, eliminating functional NMDARs prevented the loss of mIPSCs. Frequency and amplitude of mIPSCs in the dorsal horn of $Grin1^{flox/flox}$ mice injected with AAV8-*GFP-Cre* were indistinguishable from currents recorded in uninjured C57BL/6 mice, demonstrating that *Grin1* deletion preserved spinal inhibition (Figure 3F).

Fast synaptic inhibition in the spinal cord is mediated through $GABA_A$ or glycine receptors (Zeilhofer et al., 2012). For a differential evaluation of these components, we recorded GABAergic mIPSCs in the presence of the glycine receptor inhibitor strychnine (1 μM) and found that, after SNI, these mIPSCs were reduced by 56% ($p < 0.05$). The isolation of GABAergic currents further revealed a moderate decrease in amplitude by 25% ($p < 0.05$; Figure 3G). *Grin1* deletion protected against the changes in both frequency ($p < 0.01$) and amplitude ($p < 0.05$) of GABAergic mIPSCs (Figure 3H). Glycinergic mIPSCs, recorded in the presence of the $GABA_A$ receptor antagonist bicuculline (10 μM), were not affected by the nerve injury, indicating that the inhibitory deficit after SNI was primarily caused by a loss of GABAergic currents (Figure 3I).

We also tested whether excitatory currents decreased. However, neither frequency nor amplitude of miniature excitatory postsynaptic currents (mEPSCs) recorded from neurons in the L4 spinal cord of C57BL/6 mice changed after SNI (Figure S2).

The Deficit in Inhibition Is Not Explained by a Downregulation of GABA Synthesis or Vesicular Transport

The decrease in mIPSCs was greater than the proportion of inter-neurons lost after SNI. This may reflect the dense connectivity and high number of synapses formed by GABAergic neurons or suggest a deficit in transmitter synthesis and release by surviving interneurons. Gad1 and Gad2 catalyze GABA synthesis, whereas glycine is primarily recycled from the extracellular space by glycine transporter 2 (Glyt2). Viaat concentrates both GABA and glycine in presynaptic vesicles (Zeilhofer et al., 2012). To determine whether changes in the expression of these proteins contributed to the loss of inhibition, we used real-time qPCR and western blotting. Despite the reduced number of GABAergic neurons after SNI, expression of all four genes in the ipsilateral dorsal horn remained stable (Figures 4A–4D). To examine whether gene transcription was upheld by epigenomic modulation, we used chromatin immunoprecipitation (ChIP) for acetylated (ac) lysine (K) residues 9 and 27 of histone 3 (H3) and trimethylated (me3) H3K4. These histone modifications are commonly associated with active gene transcription (Kouzarides, 2007). Enrichment of H3K27ac at the start sites for *Gad1* ($p < 0.05$) and *Gad2* ($p = 0.08$) suggested enhanced transcription of these genes (Figure 4E). Consequently, *Gad1* and *Gad2* may have been upregulated in surviving GABAergic neurons without fully compensating for the effects of neurodegeneration. Other histone modifications appeared to reflect less specific changes in the dorsal horn transcriptome as they were also found at promoter regions of unrelated genes, such as *actin* (*Actb*) or *activity-regulated cytoskeletal-associated protein* (*Arc*) (Figure S3).

Eliminating NMDAR Signaling Stops the Transition to Chronic Neuropathic Pain

Stereotaxic injection of AAV8 into the dorsal horn or *GFP* expression alone did not alter nociceptive behavior except for a slightly longer response to the cooling sensation evoked by acetone evaporation (Figure S4).

To examine the impact of NMDAR elimination on pain-like behavior after SNI, we compared the responses to calibrated von Frey filaments and acetone evaporation in $Grin1^{flox/flox}$mice injected with AAV8-*GFP-Cre* or AAV8-*GFP*. Withdrawal responses in both groups of mice increased within 7 days ($p < 0.001$ compared to sham-operated mice), equivalent to the development of mechanical and cold allodynia in patients with neuropathic pain (Figure 5). Cold hypersensitivity after SNI was initially higher in mice lacking *Grin1* ($p < 0.05$ compared to $Grin1^{flox/flox}$ mice injected with AAV8-*GFP*). However, the responses of $Grin1^{flox/flox}$ mice injected with AAV8-*GFP-Cre* to both mechanical and cold stimulation returned to pre-injury levels, whereas neuropathic-pain-like behavior in mice with intact NMDARs persisted throughout the testing period of 8 weeks. Interestingly, the time to full recovery differed between stimulation modalities. Mechanical pain hypersensitivity in $Grin1^{flox/flox}$ mice injected with AAV8-*GFP-Cre* was completely reversed 3 weeks after SNI ($p < 0.001$; Figures 5A and 5B). Four weeks later, the mice no longer exhibited pain-like responses to cold stimulation ($p < 0.01$; Figures 5C and 5D).

Spinal Disinhibition and Neuropathic Pain Are Attenuated in Bax-Deficient Mice

Increased Ca^{2+} entry in response to NMDAR activation may trigger neuron death through the intrinsic apoptosis pathway. To test the role of this pathway for the loss of spinal inhibition and chronic pain after nerve injury, we used mice with a constitutive deletion of *Bax* (Knudson et al., 1995). Bax is one of the key proteins involved in intrinsic apoptosis and regulates the distribution of Ca^{2+} between cytosol and endoplasmic reticulum (D'Orsi et al., 2015).

Apoptosis after SNI was almost completely blocked in Baxdeficient mice ($Bax^{-/-}$) ($p < 0.001$; Figure 6A). Miniature IPSCs in uninjured $Bax^{-/-}$ mice were less frequent and had a lower amplitude compared to C57BL/6 mice but did not differ from wild-type mice ($Bax^{+/+}$). After SNI, the frequency of total and GABAergic mIPSCs decreased by 64% ($p < 0.05$) and 56% ($p = 0.06$), respectively, in wild-type mice, similar to the loss of inhibition in C57BL/6 mice (Figures 6B and 6C). In contrast, synaptic inhibition in $Bax^{-/-}$ mice remained intact ($p < 0.01$ for total mIPSCs and $p < 0.05$ for GABAergic currents compared to $Bax^{+/+}$ mice; Figures 6B and 6C).

Nociceptive behavior of $Bax^{-/-}$ and $Bax^{+/+}$ mice at baseline did not differ. However, painful hypersensitivity to mechanical (Figures 7A and 7B) or cold stimulation (Figures 7C and 7D) following SNI was mitigated in $Bax^{-/-}$ mice ($p < 0.001$ in a two-way ANOVA). This reduced neuropathic-pain-like behavior was observed throughout the testing period of 8 weeks. Taken together, the involvement of proapoptotic Bax in spinal disinhibition and persistent pain after SNI provided additional evidence of neurodegeneration contributing to chronic neuropathic pain (Figure S5).

DISCUSSION

Targeted deletion of functional NMDARs protected against the nerve-injury-induced loss of dorsal horn neurons, suggesting strongly that glutamate excitotoxicity caused the degeneration of these cells. Eliminating NMDAR-dependent transmission at dorsal horn synapses had surprisingly little impact on physiological nociception or the onset of pain hypersensitivity after SNI but disrupted the transition to chronic neuropathic pain. Mechanical and cold allodynia in mice lacking functional NMDARs began to resolve one week after the nerve lesion, whereas pain hypersensitivity in mice with intact glutamatergic transmission persisted for the entire testing period of 2 months. These findings suggest that NMDAR activation plays a fundamentally different role in neuropathic compared to inflammatory pain. Footpad injections of inflammatory irritants, such as capsaicin or formalin, produce NMDAR-dependent central sensitization to nociceptive stimuli within minutes (South et al., 2003), whereas NMDAR activity in the dorsal horn is not required for the maintenance of inflammatory pain (Weyerbacher et al., 2010). Nerve-injury-induced cell death is likely to involve both inhibitory and excitatory dorsal horn neurons. Here, we show that the degeneration of GABAergic neurons has major functional consequences. Neuroprotective NMDAR elimination prevented the loss of GABAergic mIPSCs and chronic pain after SNI. A constitutive deletion of proapoptotic Bax provided a similar safeguard against nerve-injury-induced disinhibition and attenuated pain-like behavior, supporting the conclusion that neurodegeneration promotes persistent neuropathic pain by

weakening the inhibitory control of nociceptive signal transmission in the superficial dorsal horn of the spinal cord.

NMDAR activation requires depolarization of the cell membrane to release a voltage-dependent Mg^{2+} block from the receptor ion channel. Enhanced nociceptive input and ectopically generated activity in injured and neighboring intact nerve fibers increase the recruitment of NMDARs at dorsal horn synapses (Kuner, 2010; Latremoliere and Woolf, 2009). An excitotoxic challenge may result directly from heightened glutamate release by primary afferents (Amir et al., 2005; Wu et al., 2001) or follow the activation of excitatory interneuron circuits within the dorsal horn (Cheng et al., 2017; Peirs et al., 2015; Duan et al., 2014; Lu et al., 2013). Insufficient glutamate uptake and presynaptic facilitation of transmitter release further increase the risk of glutamate accumulation after nerve injury (Yan et al., 2013; Inquimbert et al., 2012). Even a moderate buildup of glutamate may cause neuro-degeneration through the activation of extrasynaptic NMDARs (Bao et al., 2009; Hardingham et al., 2002). Ultimately, excitotoxic cell death is triggered by excess Ca^{2+} influx through NMDARs and subsequent activation of neuronal nitric oxide synthase (Hara and Snyder, 2007). Our results indicate a downstream engagement of the intrinsic apoptotic pathway, which involves mitochondrial translocation of Bax or Bcl2-antagonist killer 1 (Bak1) followed by cytochrome *c* release into the cytoplasm and caspase activation (Youle and Strasser, 2008). Bax may further promote excitotoxicity by regulating the Ca^{2+} exchange between cytosol and endoplasmic reticulum (D'Orsi et al., 2015).

Spatially restricted elimination of NMDAR-mediated transmission was necessary to clarify the functional significance of gluta-mate-induced neurodegeneration in the dorsal horn. NMDARs are expressed at excitatory synapses throughout the CNS. Pharmacological studies based on the use of NMDAR antagonists cannot distinguish between analgesic effects achieved by blocking postsynaptic receptors in spinal or supraspinal pathways involved in the processing of pain or by inhibiting presynaptic receptors at the central terminals of primary afferents (Yan et al., 2013; Suzuki et al., 2002). Interpreting pain-like behavior in mice treated with NMDAR antagonists is further complicated by motor side effects and the attenuation of stress, fear, and depression. Targeted *Grin1* deletion in dorsal horn neurons enabled us to reveal the role of neurodegeneration in the spinal cord for the transition from acute to chronic neuropathic pain. Pain after nerve injury appeared to evolve in three phases. (1) In the acute period of approximately 7 days, hypersensitivity to mechanical and thermal stimulation emerged independently of NMDAR expression. The initial increase in pain sensitivity must therefore be mediated primarily by glutamate signaling through AMPARs and group I mGluRs or signaling pathways involving peptide transmitters. In mice with intact NMDARs, withdrawal responses remained high as previously described (Decosterd and Woolf, 2000). (2) In the absence of NMDAR-mediated glutamatergic transmission, pain sensitivity returned to baseline levels within 3–7 weeks, demonstrating that NMDAR activity is required for the establishment of persistent neuropathic pain. The time to complete recovery may delineate the period during which neuropathic pain normally progresses to (3) the final phase of chronic pain. It is unclear why this transition period differed for mechanical and cold allodynia. One possible explanation is the high proportion of cold-sensitive C fiber afferents with increased activity after nerve injury, which may slow the resolution of cold-evoked pain (Jänig et al., 2009; Wu et al.,

2001). Loss of GABAergic neurons in laminae I+II will directly affect the inhibitory control of input from these afferents (Peirs and Seal, 2016). In contrast, the survival of inhibitory neurons in laminae III+IV may facilitate the recovery of normal thresholds for mechanically evoked pain, because these interneurons control polysynaptic connections between touch-sensitive A fiber afferents and neurons in lamina I that convey nociceptive input to the brain (Cui et al., 2016; Foster et al., 2015; Petitjean et al., 2015; Duan et al., 2014; Lu et al., 2013). It should be noted that NMDAR deletion may have interfered with mechanisms unrelated to neurodegeneration, for example, synaptic plasticity. This would offer one explanation for the difference between the behavioral phenotypes of *Grin1*$^{flox/flox}$ mice lacking functional NMDARs and *Bax*$^{-/-}$ mice. Alternatively, Bax-independent cell death pathways may be responsible for the incomplete prevention of persistent pain-like behavior in *Bax*$^{-/-}$ mice (Youle and Strasser, 2008).

The anatomical distribution of nerve-injury-induced neurode-generation suggests differences in the risk of NMDAR-mediated cell death. Apoptosis induction was concentrated in the medial dorsal horn, which receives afferent input from the injured sciatic nerve branches (Corder et al., 2010). Furthermore, a larger proportion of neurons (25%) were lost in the superficial dorsal horn compared to laminae III+IV (14%). Laminae I+II receive afferent input from nociceptive C and Ad nerve fibers. Ectopic activity in these nerve fibers is common after nerve injury (Jänig et al., 2009; Wu et al., 2001). Moreover, non-nociceptive Aβ fibers gain access to superficial dorsal horn layers as normally suppressed polysynaptic pathways open (Cheng et al., 2017; Peirs et al., 2015; Duan et al., 2014; Lu et al., 2013). This additional input involves NMDAR activation, heightening the risk of glutamate toxicity (Torsney and MacDermott, 2006). A lower exposure of inhibitory neurons in laminae III and deeper to such increases in glutamatergic input may explain the preserved integrity of glycinergic inhibition. Neurons releasing glycine, either in conjunction with GABA or as their sole neurotransmitter, reside in this region of the dorsal horn. Their number did not decline after SNI (Lu et al., 2013; Zeilhofer et al., 2005). Our findings correspond to the recently reported survival of parvalbumin-expressing inhibitory neurons at the border between inner lamina II and III (Petit-jean et al., 2015) and the pattern of neurodegeneration in the dorsal horn observed after spinal nerve ligation (Yowtak et al., 2013).

Similar to immunohistochemical studies of the rat dorsal horn (Todd, 2010), we identified 35% of neurons in laminae I+II and 40% in laminae III+IV of uninjured mice as inhibitory neurons based on the expression of fluorescent reporter proteins under the *Gad1* or *Viaat* promoter. Degeneration of these important gatekeepers of nociceptive pathways has substantial functional consequences, as the decrease in inhibitory currents after SNI demonstrates. It is not too surprising that the reduction of mIPSCs was proportionally larger than the loss of GABAergic neurons. Stereological neuron counts do not reflect the extent of changes in synaptic connections or their functional implications. They do not reveal the decay of dendrites, dendritic spines, or axon terminals associated with neurodegeneration (Lorenzo et al., 2014; Bao et al., 2009). Moreover, excess gluta-mate may have impaired the functioning of surviving neurons.

The neuroprotective effect of *α*-phenyl-*N*-*tert*-butylnitrone, a compound that traps free radical species and inhibits their synthesis, suggests that oxidative stress is one consequence

of NMDAR-mediated excitotoxicity in the dorsal horn (Yowtak et al., 2013). Other mechanisms are likely to contribute to the decrease in synaptic inhibition after nerve injury. Brain-derived neurotrophic factor (Bdnf) released from microglia provokes downregulation of K^+-Cl^- cotransporter 2 (KCC2). Reduced KCC2 expression, phosphorylation, and cleavage of the transporter by the Ca^{2+}-dependent protease calpain lead to a rise in intracellular Cl^- that weakens the hyperpolarizing efficacy of $GABA_A$ receptor activation (Kahle et al., 2016; Zhou et al., 2012; Coull et al., 2005). The functional significance of these mechanisms changes with time. Microglial activity, for example, is high during the onset of neuropathic pain. Consequently, KCC2 regulation by Bdnf is probably less relevant for chronic pain (Peng et al., 2016). In contrast, the NMDAR-dependent degeneration of GABAergic neurons contributes specifically to the persistence of neuropathic pain.

We conclude that chronic neuropathic pain resembles, in a key aspect of its pathophysiology, a neurodegenerative disorder. Cell death induction after nerve injury appears to be a protracted process in which a relatively low level of apoptosis leads to a sizable decrease in the number of dorsal horn neurons over time. This slow progression is comparable to neurodegeneration in other diseases associated with chronic glutamate toxicity, such as amyotrophic lateral sclerosis (Lewerenz and Maher, 2015). The irreversible loss of GABAergic neurons causes a major shift in the normally carefully regulated balance between inhibitory and excitatory modulation of pain processing. This long-term deficit in the control of nociceptive signaling is likely to contribute to the difficulty of treating neuropathic pain. On the other hand, neuroprotection, which we accomplished through targeted elimination of NMDAR-mediated glutamatergic transmission and deletion of proapoptotic Bax, may provide an opportunity for the prevention of chronic pain. Mechanism-based treatment approaches for neuropathic pain are urgently needed (Colloca et al., 2017). Our findings strengthen the rationale for strategies aiming to restore GABAergic inhibition through gene transfer (Hao et al., 2005) or the transplantation of GABAergic neuron precursors (Bráz et al., 2012).

Supplementary Material

Refer to Web version on PubMed Central for supplementary material.

EXPERIMENTAL PROCEDURES

In compliance with the Animal Research: Reporting of *In Vivo* Experiments (ARRIVE) guidelines, mice were randomly allocated to the experimental conditions and investigators blind to the allocation. A detailed description of the Experimental Procedures is provided in the Supplemental Information.

Animals

This study was conducted in accordance with the NIH Guide for the Care and Use of Laboratory Animals and approved by the Institutional Animal Care and Use Committees (IACUCs) of Columbia University and Boston Children’s Hospital.

Experiments were performed with male adult (8–12 weeks old) animals. C57BL/6 and *Bax*$^{-/-}$ mice (Knudson et al., 1995) were purchased from Jackson Laboratory. *Grin1*$^{flox/flox}$, *Gad1-GFP*, and *Viaat-Venus* mice have been described (Wang et al., 2009; Tamamaki et al., 2003; Tsien et al., 1996).

Surgery

For SNI, we ligated and transected the common peroneal and tibial branches of the sciatic nerve (Decosterd and Woolf, 2000). Mice received 2 unilateral (left) stereotaxic injections of AAV8 vectors expressing *GFP* or *GFP-Cre* into the dorsal horn, cranial, and caudal of spinal cord segment L4, as previously described (Inquimbert et al., 2013).

TUNEL Assay

We used ApopTag *In Situ* Apoptosis Detection Kits (EMD Millipore) for TUNEL on cryosections (10 μm) of the dorsal horn. Only profiles exhibiting chromatin changes indicative of apoptosis (pyknosis, fragmentation, and marginalization) were counted.

Stereology

For the stereological analysis of total neurons, we cut transverse cryosections (50 μm) of the spinal cord. From a random start, we selected every 4th section and stained them for NeuN (EMD Millipore). Neurons were counted in laminae I+II and laminae III+IV of the medial half of the dorsal horn. Dorsal and ventral boundaries of these regions of interest (ROIs) were defined based on cytoarchitecture. The number of neurons was determined using the optical fractionator (West et al., 1991), with counting spaces distributed in a systematic-random fashion (Table S1). The analysis was performed with Stereo Investigator software (MBF Bioscience).

Inhibitory neurons expressing GFP or Venus were counted in sections of 30-μm thickness. We selected every 5th section and immunostained them for NeuN and the γ isoform of protein kinase C (PKCγ) (Santa Cruz Biotechnology), using fluorescently labeled secondary antibodies for detection. We delineated the same ROIs as for the counts of total neurons based on cytoarchitecture and PKCγ expression, which demarcates the boundary between laminae II and III (Table S1).

qPCR

RNA was purified from the ipsilateral dorsal quadrants of the L4 spinal cord. qPCR was performed with a SYBR Select Master Mix (Thermo Fisher Scientific) except for Glyt2 (*Slc6a5*). For *Slc6a5*, we utilized a TaqMan Universal Mastermix II (Thermo Fisher Scientific) and FAM dye-labeled minor groove-binding (MGB) probes. Targets were normalized to *glyceraldehyde-3-phosphate dehydrogenase* (*Gapdh*). Table S2 lists the forward and reverse primers. All reactions were performed on a StepOnePlus System (Thermo Fisher Scientific).

ChIP

For ChIP assays, we combined the left (ipsilateral) dorsal quadrants of the L4 spinal cord of two mice into one sample. ChIP was performed as previously described (Korb et al., 2015).

Three technical replicates were averaged for each biologically independent sample and DNA levels normalized to input. Table S2 lists the forward and reverse primers.

In Situ Hybridization

Riboprobes of 911 bp length were generated from a *Grin1* cDNA template and labeled with digoxigenin (Roche Life Science). Probes bound to spinal cord cryosections (10 μm) were immunostained with antigen-binding fragments (Fabs) conjugated to alkaline phosphatase (Roche Life Science). Probes in sense orientation served as negative controls.

Electrophysiology

Recordings were performed on acute spinal cord slices as described (Inquim-bert et al., 2012; Tong and MacDermott, 2014). We obtained voltage-clamp whole-cell patch recordings from dorsal horn neurons in lamina II and the border between laminae II and III. We recorded mIPSCs at a holding potential of −70 mV in the presence of 0.5 μM tetrodotoxin (TTX) and ionotropic glutamate receptor blockers, either 2 mM kynurenic acid or 50 μM D-2-amino-5-phosphonovalerate (AP5) and 10 μM 2,3-dioxo-6-nitro-1,2,3,4-tetrahydrobenzo[f]quinoxaline-7-sulfonamide (NBQX). To isolate GABAergic or glycinergic currents, we used 1 μM strychnine HCl or 10 μM bicuculline methiodide, respectively. Miniature EPSCs were recorded at −70 mV in the presence of 0.5 μM TTX, 1 μM strychnine, and 10 μM bicuculline. Currents evoked by 100 μM NMDA were recorded at +40 mV in the presence of 25 mM NBQX. We used pClamp10 software (Molecular Devices) for data acquisition and Mini Analysis software (Synaptosoft) or the Win EDR and Win WCP programs of Strathclyde Electro-physiology Software for analysis.

Behavioral Tests

All behavioral evaluations were replicated in two independent groups of animals. We applied calibrated von Frey filaments in the territory of the spared sural nerve to determine the mechanical withdrawal threshold. To test for cold sensitivity, we recorded the withdrawal duration after applying a drop of acetone to the skin, which produces a cool sensation upon evaporation (Inquimbert et al., 2012). Technical details of the tests for mechanical hyperalgesia and heat-induced pain are provided in the Supplemental Experimental Procedures.

Statistics

We used an unpaired two-sided Student’s t test for comparing two experimental conditions, a one-way ANOVA followed by Dunnett’s or Tukey’s test for comparing more than two conditions, and a two-way ANOVA followed by Sidak’s or Bonferroni’s test for comparing experimental conditions over time. We utilized Prism software (GraphPad) for these tests. Sample sizes provided ≥90% power for statistically significant results at $\alpha = 0.05$, as calculated with G*Power software (Heinrich Heine University Düsseldorf). Unless otherwise mentioned, data are represented as mean ± SEM.

ACKNOWLEDGMENTS

We thank Susumu Tonegawa for providing the *Grin1*$^{flox/flox}$ mice, Brian K. Kaspar for the *GFP-Cre* plasmid, Christoph Kellendonk and David V. Pow for the antibodies targeting Cre and glycine, respectively, and John Dempster for the Win EDR and Win WCP programs of Strathclyde Electrophysiology Software. We further thank Amy B. MacDermott and Christoph Kellendonk for helpful comments on the manuscript. This work was supported by a grant from the National Institute of Neurological Disorders and Stroke (R01 NS050408) to J.S. and an MD fellowship from the Boehringer Ingelheim Fonds to M.M.

REFERENCES

Amir R, Kocsis JD, and Devor M (2005). Multiple interacting sites of ectopic spike electrogenesis in primary sensory neurons. J. Neurosci 25, 2576–2585. [PubMed: 15758167]

Bao X, Pal R, Hascup KN, Wang Y, Wang WT, Xu W, Hui D, Agbas A, Wang X, Michaelis ML, et al. (2009). Transgenic expression of Glud1 (glutamate dehydrogenase 1) in neurons: in vivo model of enhanced glutamate release, altered synaptic plasticity, and selective neuronal vulnerability.J. Neurosci 29, 13929–13944. [PubMed: 19890003]

Bráz JM, Sharif-Naeini R, Vogt D, Kriegstein A, Alvarez-Buylla A, Rubenstein JL, and Basbaum AI (2012). Forebrain GABAergic neuron precursors integrate into adult spinal cord and reduce injury-induced neuropathic pain. Neuron 74, 663–675. [PubMed: 22632725]

Cheng L, Duan B, Huang T, Zhang Y, Chen Y, Britz O, Garcia-Camp-many L, Ren X, Vong L, Lowell BB, et al. (2017). Identification of spinal circuits involved in touch-evoked dynamic mechanical pain. Nat. Neurosci 20, 804–814. [PubMed: 28436981]

Colloca L, Ludman T, Bouhassira D, Baron R, Dickenson AH, Yarnitsky D, Freeman R, Truini A, Attal N, Finnerup NB, et al. (2017). Neuropathic pain. Nat. Rev. Dis. Primers 3, 17002. [PubMed: 28205574]

Corder G, Siegel A, Intondi AB, Zhang X, Zadina JE, and Taylor BK (2010). A novel method to quantify histochemical changes throughout the mediolateral axis of the substantia gelatinosa after spared nerve injury: characterization with TRPV1 and substance P. J. Pain 11, 388–398. [PubMed: 20350706]

Coull JA, Beggs S, Boudreau D, Boivin D, Tsuda M, Inoue K, Gravel C, Salter MW, and De Koninck Y (2005). BDNF from microglia causes the shift in neuronal anion gradient underlying neuropathic pain. Nature 438, 1017–1021. [PubMed: 16355225]

Cui L, Miao X, Liang L, Abdus-Saboor I, Olson W, Fleming MS, Ma M, Tao YX, and Luo W (2016). Identification of Early RET+ Deep Dorsal Spinal Cord Interneurons in Gating Pain. Neuron 91, 1137–1153. [PubMed: 27545714]

D'Orsi B, Kilbride SM, Chen G, Perez Alvarez S, Bonner HP, Pfeiffer S, Plesnila N, Engel T, Henshall DC, Düssmann H, and Prehn JH (2015). Bax regulates neuronal Ca2+ homeostasis. J. Neurosci 35, 1706–1722. [PubMed: 25632145]

Decosterd I, and Woolf CJ (2000). Spared nerve injury: an animal model of persistent peripheral neuropathic pain. Pain 87, 149–158. [PubMed: 10924808]

Duan B, Cheng L, Bourane S, Britz O, Padilla C, Garcia-Campmany L, Krashes M, Knowlton W, Velasquez T, Ren X, et al. (2014). Identification of spinal circuits transmitting and gating mechanical pain. Cell 159, 1417–1432. [PubMed: 25467445]

Foster E, Wildner H, Tudeau L, Haueter S, Ralvenius WT, Jegen M, Johannssen H, Hösli L, Haenraets K, Ghanem A, et al. (2015). Targeted ablation, silencing, and activation establish glycinergic dorsal horn neurons as key components of a spinal gate for pain and itch. Neuron 85, 1289–1304. [PubMed: 25789756]

Hao S, Mata M, Wolfe D, Huang S, Glorioso JC, and Fink DJ (2005). Gene transfer of glutamic acid decarboxylase reduces neuropathic pain. Ann. Neurol 57, 914–918. [PubMed: 15929041]

Hara MR, and Snyder SH (2007). Cell signaling and neuronal death. Annu. Rev. Pharmacol. Toxicol 47, 117–141. [PubMed: 16879082]

Hardingham GE, Fukunaga Y, and Bading H (2002). Extrasynaptic NMDARs oppose synaptic NMDARs by triggering CREB shut-off and cell death pathways. Nat. Neurosci 5, 405–414. [PubMed: 11953750]

Inquimbert P, Bartels K, Babaniyi OB, Barrett LB, Tegeder I, and Scholz J (2012). Peripheral nerve injury produces a sustained shift in the balance between glutamate release and uptake in the dorsal horn of the spinal cord. Pain 153, 2422–2431. [PubMed: 23021150]

Inquimbert P, Moll M, Kohno T, and Scholz J (2013). Stereotaxic injection of a viral vector for conditional gene manipulation in the mouse spinal cord. J. Vis. Exp, e50313. [PubMed: 23542888]

Jänig W, Grossmann L, and Gorodetskaya N (2009). Mechano- and thermosensitivity of regenerating cutaneous afferent nerve fibers. Exp. Brain Res 196, 101–114. [PubMed: 19139872]

Ji RR, Xu ZZ, and Gao YJ (2014). Emerging targets in neuroinflammation-driven chronic pain. Nat. Rev. Drug Discov 13, 533–548. [PubMed: 24948120]

Kahle KT, Schmouth JF, Lavastre V, Latremoliere A, Zhang J, Andrews N, Omura T, Laganière J, Rochefort D, Hince P, et al. (2016). Inhibition of the kinase WNK1/HSN2 ameliorates neuropathic pain by restoring GABA inhibition. Sci. Signal 9, ra32. [PubMed: 27025876]

Knudson CM, Tung KS, Tourtellotte WG, Brown GA, and Korsmeyer SJ (1995). Bax-deficient mice with lymphoid hyperplasia and male germ cell death. Science 270, 96–99. [PubMed: 7569956]

Korb E, Herre M, Zucker-Scharff I, Darnell RB, and Allis CD (2015). BET protein Brd4 activates transcription in neurons and BET inhibitor Jq1 blocks memory in mice. Nat. Neurosci 18, 1464–1473. [PubMed: 26301327]

Kouzarides T (2007). Chromatin modifications and their function. Cell 128, 693–705. [PubMed: 17320507]

Kuner R (2010). Central mechanisms of pathological pain. Nat. Med 16, 1258–1266. [PubMed: 20948531]

Latremoliere A, and Woolf CJ (2009). Central sensitization: a generator of pain hypersensitivity by central neural plasticity. J. Pain 10, 895–926. [PubMed: 19712899]

Lewerenz J, and Maher P (2015). Chronic Glutamate Toxicity in Neurode-generative Diseases-What is the Evidence? Front. Neurosci 9, 469. [PubMed: 26733784]

Lorenzo LE, Magnussen C, Bailey AL, St Louis M, De Koninck Y, and Ribeiro-da-Silva A (2014). Spatial and temporal pattern of changes in the number of GAD65-immunoreactive inhibitory terminals in the rat superficial dorsal horn following peripheral nerve injury. Mol. Pain 10, 57. [PubMed: 25189404]

Lu Y, Dong H, Gao Y, Gong Y, Ren Y, Gu N, Zhou S, Xia N, Sun YY, Ji RR, and Xiong L (2013). A feed-forward spinal cord glycinergic neural circuit gates mechanical allodynia. J. Clin. Invest 123, 4050–4062. [PubMed: 23979158]

Peirs C, and Seal RP (2016). Neural circuits for pain: Recent advances and current views. Science 354, 578–584. [PubMed: 27811268]

Peirs C, Williams SP, Zhao X, Walsh CE, Gedeon JY, Cagle NE, Goldring AC, Hioki H, Liu Z, Marell PS, and Seal RP (2015). Dorsal Horn Circuits for Persistent Mechanical Pain. Neuron 87, 797–812. [PubMed: 26291162]

Peng J, Gu N, Zhou L, B Eyo U, Murugan M, Gan WB, and Wu LJ (2016). Microglia and monocytes synergistically promote the transition from acute to chronic pain after nerve injury. Nat. Commun 7, 12029. [PubMed: 27349690]

Petitjean H, Pawlowski SA, Fraine SL, Sharif B, Hamad D, Fatima T, Berg J, Brown CM, Jan LY, Ribeiro-da-Silva A, et al. (2015). Dorsal Horn Parvalbumin Neurons Are Gate-Keepers of Touch-Evoked Pain after Nerve Injury. Cell Rep. 13, 1246–1257. [PubMed: 26527000]

Polgár E, Hughes DI, Riddell JS, Maxwell DJ, Puskár Z, and Todd AJ (2003). Selective loss of spinal GABAergic or glycinergic neurons is not necessary for development of thermal hyperalgesia in the chronic constriction injury model of neuropathic pain. Pain 104, 229–239. [PubMed: 12855333]

Polgár E, Gray S, Riddell JS, and Todd AJ (2004). Lack of evidence for significant neuronal loss in laminae I-III of the spinal dorsal horn of the rat in the chronic constriction injury model. Pain 111, 144–150. [PubMed: 15327818]

Polgár E, Hughes DI, Arham AZ, and Todd AJ (2005). Loss of neurons from laminas I-III of the spinal dorsal horn is not required for development of tactile allodynia in the spared nerve injury model of neuropathic pain. J. Neurosci 25, 6658–6666. [PubMed: 16014727]

Scholz J, and Woolf CJ (2007). The neuropathic pain triad: neurons, immune cells and glia. Nat. Neurosci 10, 1361–1368. [PubMed: 17965656]

Scholz J, Broom DC, Youn DH, Mills CD, Kohno T, Suter MR, Moore KA, Decosterd I, Coggeshall RE, and Woolf CJ (2005). Blocking caspase activity prevents transsynaptic neuronal apoptosis and the loss of inhibition in lamina II of the dorsal horn after peripheral nerve injury. J. Neurosci 25, 7317–7323. [PubMed: 16093381]

South SM, Kohno T, Kaspar BK, Hegarty D, Vissel B, Drake CT, Ohata M, Jenab S, Sailer AW, Malkmus S, et al. (2003). A conditional deletion of the NR1 subunit of the NMDA receptor in adult spinal cord dorsal horn reduces NMDA currents and injury-induced pain. J. Neurosci 23, 5031–5040. [PubMed: 12832526]

Suzuki R, Morcuende S, Webber M, Hunt SP, and Dickenson AH (2002). Superficial NK1-expressing neurons control spinal excitability through activation of descending pathways. Nat. Neurosci 5, 1319–1326. [PubMed: 12402039]

Tamamaki N, Yanagawa Y, Tomioka R, Miyazaki J, Obata K, and Kaneko T (2003). Green fluorescent protein expression and colocalization with calretinin, parvalbumin, and somatostatin in the GAD67-GFP knock-in mouse.J. Comp. Neurol 467, 60–79. [PubMed: 14574680]

Todd AJ (2010). Neuronal circuitry for pain processing in the dorsal horn. Nat. Rev. Neurosci 11, 823–836. [PubMed: 21068766]

Tong CK, and MacDermott AB (2014). Synaptic GluN2A and GluN2B containing NMDA receptors within the superficial dorsal horn activated following primary afferent stimulation. J. Neurosci 34, 10808–10820. [PubMed: 25122884]

Torsney C, and MacDermott AB (2006). Disinhibition opens the gate to pathological pain signaling in superficial neurokinin 1 receptor-expressing neurons in rat spinal cord. J. Neurosci 26, 1833–1843. [PubMed: 16467532]

Tsien JZ, Huerta PT, and Tonegawa S (1996). The essential role of hippo-campal CA1 NMDA receptor-dependent synaptic plasticity in spatial memory. Cell 87, 1327–1338. [PubMed: 8980238]

von Hehn CA, Baron R, and Woolf CJ (2012). Deconstructing the neuropathic pain phenotype to reveal neural mechanisms. Neuron 73, 638–652. [PubMed: 22365541]

Wang Y, Kakizaki T, Sakagami H, Saito K, Ebihara S, Kato M, Hirabayashi M, Saito Y, Furuya N, and Yanagawa Y (2009). Fluorescent labeling of both GABAergic and glycinergic neurons in vesicular GABA transporter (VGAT)-venus transgenic mouse. Neuroscience 164, 1031–1043. [PubMed: 19766173]

West MJ, Slomianka L, and Gundersen HJ (1991). Unbiased stereological estimation of the total number of neurons in thesubdivisions of the rat hippo-campus using the optical fractionator. Anat. Rec 231, 482–497. [PubMed: 1793176]

Weyerbacher AR, Xu Q, Tamasdan C, Shin SJ, and Inturrisi CE (2010). N-Methyl-D-aspartate receptor (NMDAR) independent maintenance of inflammatory pain. Pain 148, 237–246. [PubMed: 20005044]

Wu G, Ringkamp M, Hartke TV, Murinson BB, Campbell JN, Griffin JW, and Meyer RA (2001). Early onset of spontaneous activity in uninjured C-fiber nociceptors after injury to neighboring nerve fibers. J. Neurosci 21, RC140. [PubMed: 11306646]

Yan X, Jiang E, Gao M, and Weng HR (2013). Endogenous activation of presynaptic NMDA receptors enhances glutamate release from the primary afferents in the spinal dorsal horn in a rat model of neuropathic pain. J. Physiol 591, 2001–2019. [PubMed: 23359671]

Youle RJ, and Strasser A (2008). The BCL-2 protein family: opposing activities that mediate cell death. Nat. Rev. Mol. Cell Biol 9, 47–59. [PubMed: 18097445]

Yowtak J, Wang J, Kim HY, Lu Y, Chung K, and Chung JM (2013). Effect of antioxidant treatment on spinal GABA neurons in a neuropathic pain model in the mouse. Pain 154, 2469–2476. [PubMed: 23880056]

Zeilhofer HU, Studler B, Arabadzisz D, Schweizer C, Ahmadi S, Layh B, Bösl MR, and Fritschy JM (2005). Glycinergic neurons expressing enhanced green fluorescent protein in bacterial artificial chromosome transgenic mice. J. Comp. Neurol 482, 123–141. [PubMed: 15611994]

Zeilhofer HU, Wildner H, and Yévenes GE (2012). Fast synaptic inhibition in spinal sensory processing and pain control. Physiol. Rev 92, 193–235. [PubMed: 22298656]

Zhou HY, Chen SR, Byun HS, Chen H, Li L, Han HD, Lopez-Berestein G, Sood AK, and Pan HL (2012). N-methyl-D-aspartate receptor-and calpain-mediated proteolytic cleavage of K+-Cl-

cotransporter-2 impairs spinal chloride homeostasis in neuropathic pain. J. Biol. Chem 287, 33853–33864. [PubMed: 22854961]

Highlights

- Nerve injury provokes excitotoxic cell death in the dorsal horn of the spinal cord
- Degeneration of GABAergic interneurons leads to a marked decrease in mIPSCs
- Targeted deletion of NMDA receptors or Bax knockout prevents the loss of inhibition
- Neuroprotection blocks the transition of acute to chronic neuropathic pain

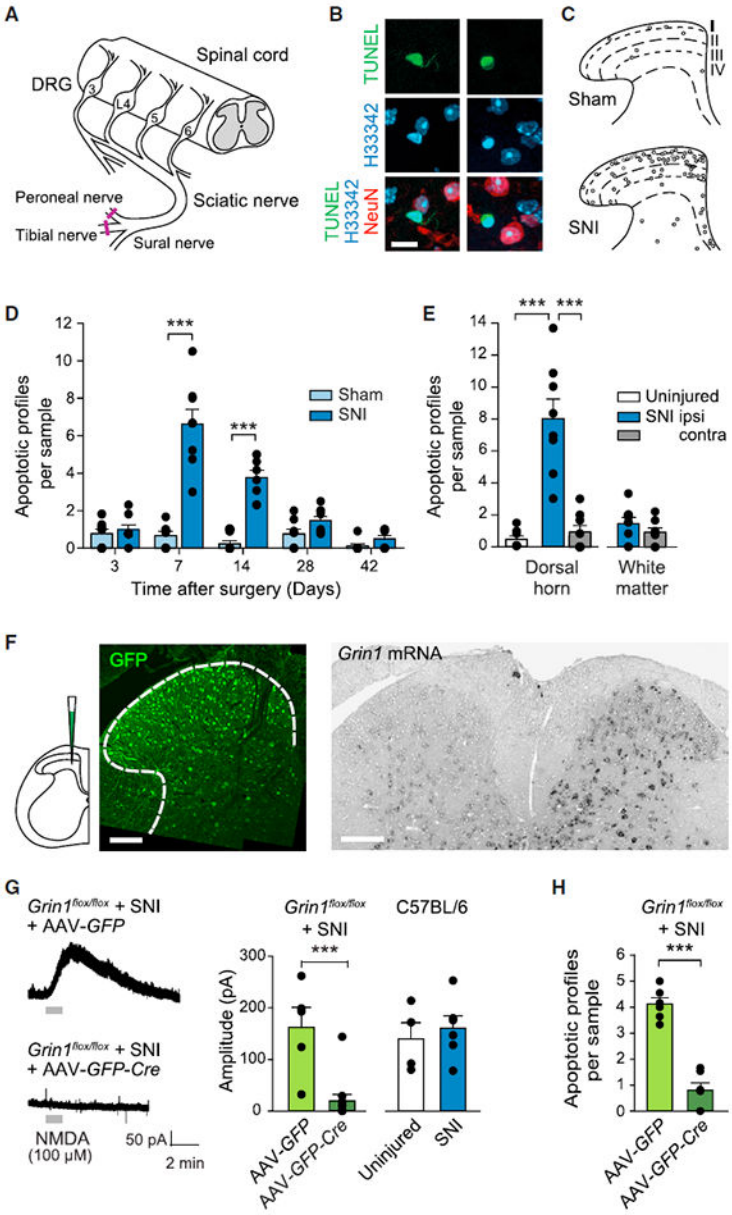

Figure 1. NMDAR-Mediated Glutamatergic Transmission Causes Nerve-Injury-Induced Apoptosis

(A) Schematic illustration of SNI and the relevant neuroanatomy. DRG, dorsal root ganglion.

(B) Apoptotic cell profiles 7 days after SNI. H33342, Hoechst 33342 (bisbenzimide). Scale bar, 10 µm.

(C) Distribution of apoptotic profiles within the dorsal horn, shown in overlays of 10 sections per mouse (n = 8 mice).

(D) Time course of apoptosis induction. Apoptotic profiles were counted in 10 sections per mouse (n = 8). $p < 0.001$ for surgery and time in a two-way ANOVA. ***$p < 0.001$ in Sidak's test following the ANOVA.

(E) Apoptosis in uninjured mice and the ipsilateral and contralateral dorsal horns of mice 7 days after SNI (n = 8). $p < 0.001$ in a one-way ANOVA. ***p <0.001 in Dunnett's test following the ANOVA. Apoptosis in the white matter was not significantly different in Student's t test.

(F and G) Stereotaxic injection of AAV8-*GFP-Cre* into the spinal cord of *Grin1*$^{flox/flox}$ mice eliminated NMDAR function.

(F) GFP expression (left) and *in situ* hybridization of *Grin1* mRNA (right) 3 weeks after injection of the vector into the left dorsal horn of the lumbar (L4) spinal cord. Scale bars, 100 μm (left) or 200 μm (right).

(G) Excitatory currents evoked by NMDA (100 μM) in *Grin1*$^{flox/flox}$ mice injected with AAV8-*GFP* or AAV8-*GFP-Cre*. SNI was performed 2 or 3 weeks after the vector injection. Two weeks after the nerve injury, we compared current amplitudes in the dorsal horn of mice injected with AAV8-*GFP* (n = 5 neurons) or AAV8-*GFP-Cre* (n = 11). ***p <0.001 in Student's t test. Currents recorded in *Grin1*$^{flox/flox}$ mice injected with AAV8-*GFP* did not differ from those in uninjured C57BL/6 mice (n = 4) or C57BL/6 mice after SNI (n = 6).

(H) Apoptotic profiles 7 days after SNI in the dorsal horn of *Grin1*$^{flox/flox}$ mice injected with AAV8-*GFP* or AAV8-*GFP-Cre* (n = 6 mice). ***p < 0.001 in Student's t test.

Error bars indicate SEM. See also Figures S1 and S5.

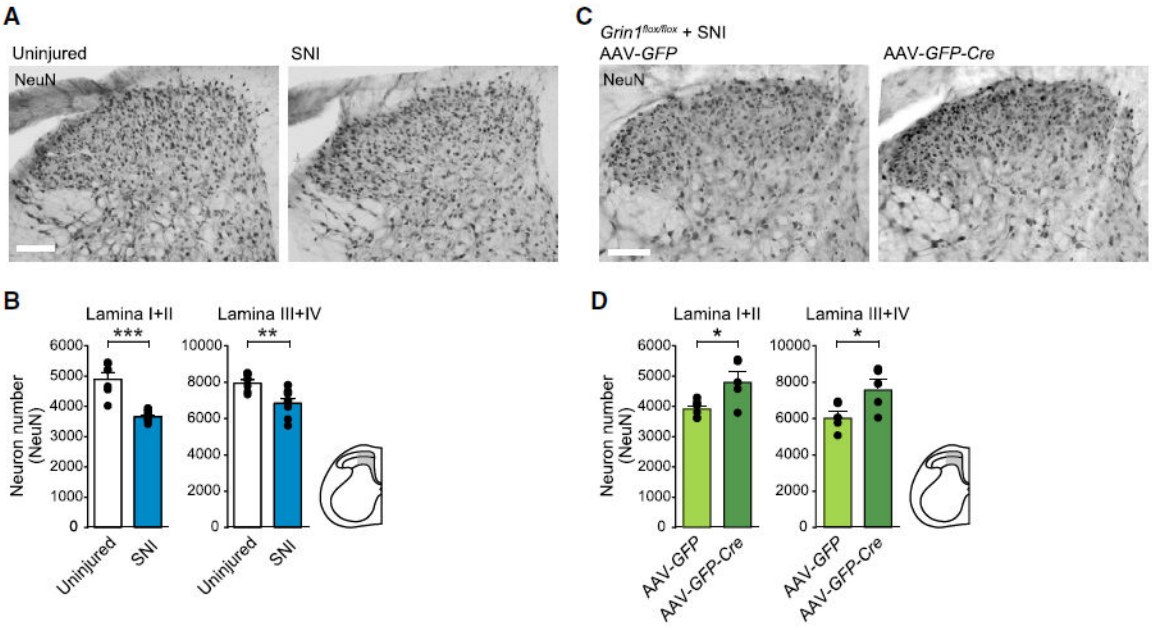

Figure 2. *Grin1* Deletion Protects against the Loss of Dorsal Horn Neurons

(A) Representative photographs of the L4 dorsal horn of uninjured C57BL/6 mice and 28 days after SNI. Neurons were immunostained for NeuN. Scale bar, 100 μm.

(B) Stereological counts of neurons (NeuN) in laminae I+II and laminae III+IV of the dorsal horn of uninjured mice (n = 6) and after SNI (n = 8).

(C) Representative photographs of the L4 dorsal horn of *Grin1*$^{flox/flox}$ mice 28 days after SNI. Scale bar, 100 μm.

(D) Stereological counts of neurons in the dorsal horn of *Grin1*$^{flox/flox}$ mice injected with AAV8-*GFP* (n = 6) or AAV8-*GFP-Cre* (n = 5). Neurons were counted 28 days after SNI. *p < 0.05; **p < 0.01; ***p < 0.001 in Student's t tests. Error bars indicate SEM. Schematic drawings indicate the counting ROIs (gray). See also Table S1.

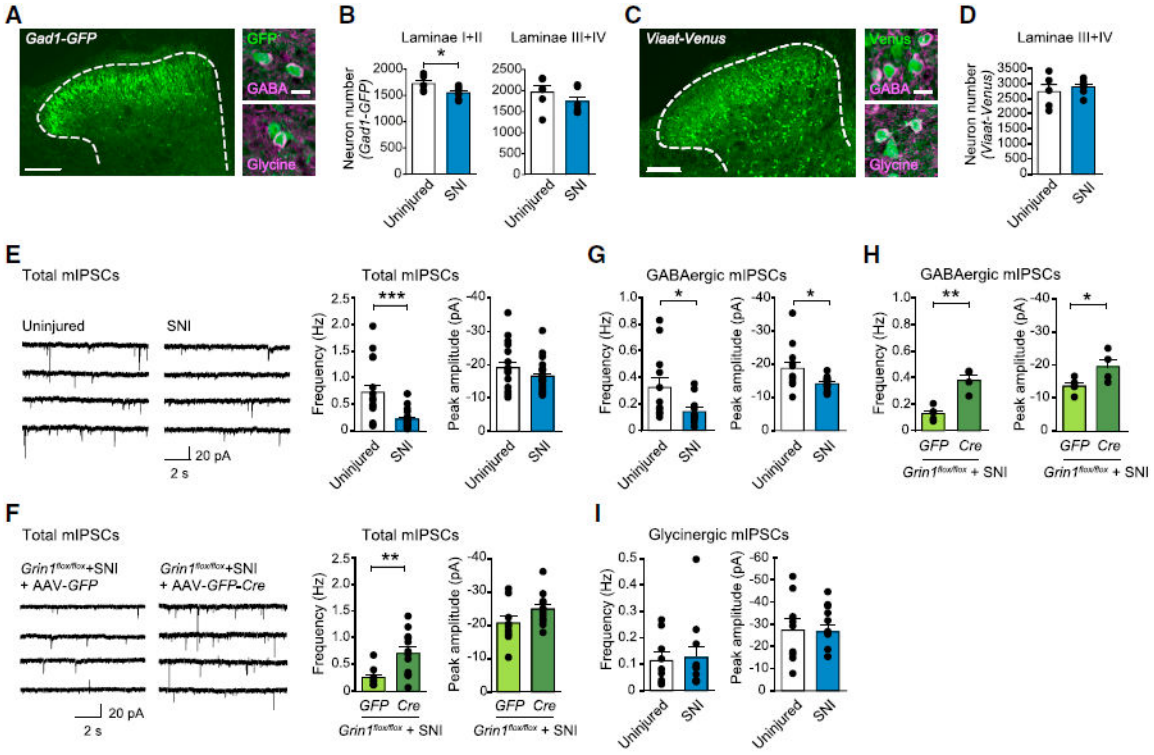

Figure 3. Neuroprotection Preserves Spinal Inhibition

(A) GFP expression in GABAergic dorsal horn neurons of *Gad1-GFP* mice. Some GABAergic neurons also produced glycine. Scale bars, 100 μm (large panels) or 10 μm (small panels).

(B) Stereological counts of GABAergic neurons in the L4 dorsal horn of uninjured *Gad1-GFP* mice and 28 days after SNI (n = 6 mice).

(C) *Viaat-Venus* mice expressed the fluorescent protein in both GABAergic and glycinergic neurons. Scale bars, 100 μm (large panels) or 10 μm (small panels).

(D) Stereological counts of inhibitory interneurons in laminae III+IV of uninjured *Viaat-Venus* mice (n = 5) and 28 days after SNI (n = 6).

(E–I) Miniature IPSC recordings.

(E) Representative traces of total mIPSCs in C57BL/6 mice. Bar graphs show current frequency and peak amplitude in uninjured mice (n = 17 neurons) and 2 weeks after SNI (n = 25).

(F) Comparison of total mIPSCs in the spinal cord of *Grin1*$^{flox/flox}$ mice injected with AAV8-*GFP* (n = 8 neurons) or AAV8-*GFP-Cre* (n = 12). Currents were recorded 2 weeks after SNI.

(G) Frequency and peak amplitude of GABAergic mIPSCs in uninjured C57BL/6 mice (n = 12) and 2 weeks after SNI (n = 12).

(H) GABAergic mIPSCs in *Grin1*$^{flox/flox}$ mice injected with AAV8-*GFP* (n = 5) or AAV8-*GFP-Cre* (n = 4). GABAergic currents were recorded in the presence of strychnine.

(I) Glycinergic mIPSCs, recorded in the presence of bicuculline, did not differ between uninjured C57BL/6 mice (n = 9) and 2 weeks after SNI (n = 11). *p < 0.05; **p < 0.01;

***$p < 0.001$. Student's t test was used for all comparisons. Error bars indicate SEM. See also Figure S2 and Table S1.

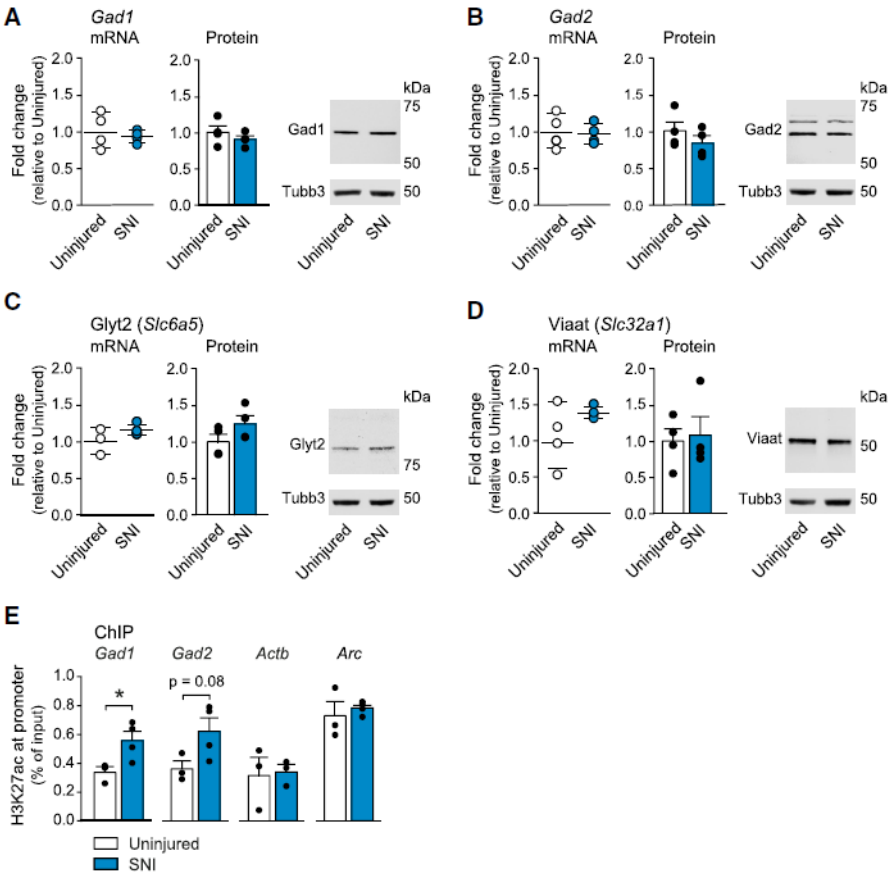

Figure 4. Surviving Neurons Maintain the Expression of Gad, Glyt2, and Viaat

(A–D) Transcript and protein levels of (A) Gad1, (B) Gad2, (C) Glyt2 (*Slc6a5*), and (D) Viaat (*Slc32a1*) were unchanged in the L4 dorsal horn of mice 28 days after SNI (n = 3 or 4 biological replicates). qPCR results are presented as mean fold change of $\Delta C_T \pm SD$ after normalization to *Gapdh* and protein levels as mean fold change ± SEM after normalization to β3-tubulin (Tubb3). Images show representative western blot results.

(E) ChIP analysis of H3K27ac at the promoter regions for *Gad1*, *Gad2*, *Actb*, and *Arc* (n = 4). His-tone modifications 28 days after SNI are shown, compared to uninjured mice.

*p < 0.05. Student's t test was used for all comparisons. Error bars indicate SEM. See also Figure S3 and Table S2.

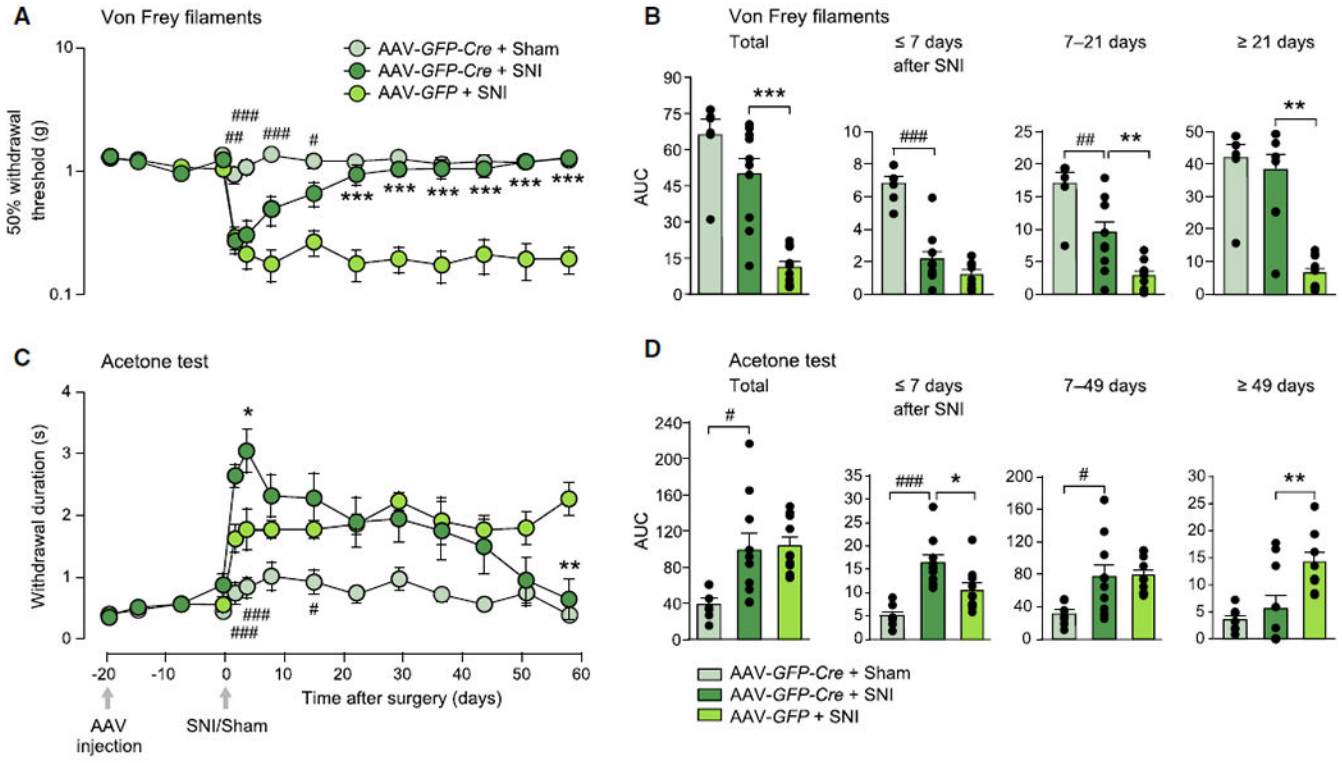

Figure 5. Eliminating Functional NMDARs in the Dorsal Horn Blocks the Transition from Acute to Chronic Neuropathic Pain

(A and C) Withdrawal responses to (A) mechanical (von Frey filaments) or (C) cold stimulation (acetone evaporation) after sham surgery (n = 7 mice) or SNI (n = 10) in *Grin1*$^{flox/flox}$ mice injected with AAV8-*GFP-Cre*, and SNI in *Grin1*$^{flox/flox}$ mice injected with AAV8-*GFP* (n = 10). Behavioral outcomes were compared using twoway ANOVAs. $p < 0.001$ for treatment and time in the responses to stimulation with von Frey filaments; $p < 0.01$ for treatment and $p < 0.001$ for time in the acetone test. Asterisks and pound signs indicate the results of Bonferroni's tests following the ANOVAs. (B and D) Areas under the curve (AUCs) were first compared for the total test duration after SNI ($p < 0.001$ for Frey filaments, B, and acetone test, D, in one-way ANOVAs). Separately, we compared AUCs in the acute phase of the first 7 days after SNI ($p < 0.001$ for both test modalities), during the transition from acute to persistent pain ($p < 0.001$ for the stimulation with von Frey filaments and $p < 0.05$ for the acetone test), and for persistent pain after 21 or 49 days, respectively ($p < 0.001$ for von Frey filaments and $p < 0.01$ for the acetone test). Asterisks and pound signs indicate the results of Tukey's tests following the ANOVAs.

*$p < 0.05$, **$p < 0.01$, and ***$p < 0.001$ for the comparison of AAV8-*GFP-Cre* + SNI and AAV8-*GFP* + SNI; $^{\#}p < 0.05$, $^{\#\#}p < 0.01$, and $^{\#\#\#}p < 0.001$ for the comparison of AAV8-*GFP-Cre* + Sham and AAV8-*GFP-Cre* + SNI. Error bars indicate SEM. See also Figure S4.

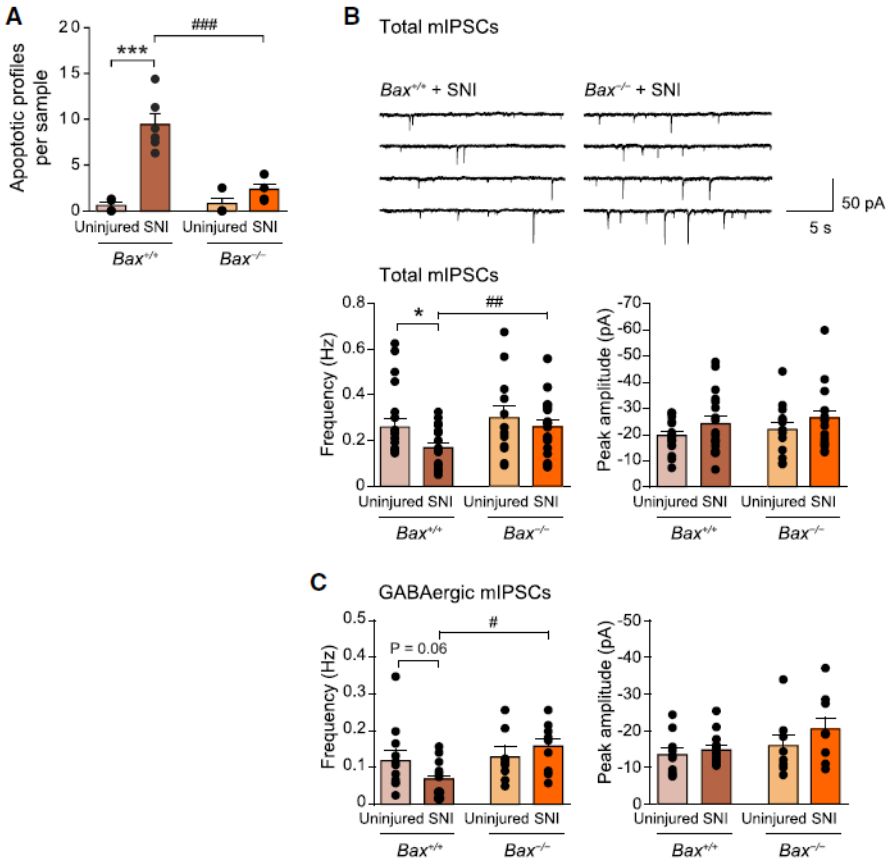

Figure 6. Mice Lacking Proapoptotic Bax Are Protected against Nerve-Injury-Induced Disinhibition

(A) Apoptotic profiles in $Bax^{+/+}$ and $Bax^{-/-}$ mice 7 days after SNI (n = 6).

(B) Representative recordings of total mIPSCs. Bar graphs below show current frequency and peak amplitude in uninjured $Bax^{+/+}$ mice and $Bax^{+/+}$ mice 2 weeks after SNI (n = 18 neurons) and in uninjured $Bax^{-/-}$ mice (n = 13) and $Bax^{-/-}$ mice 2 weeks after SNI (n = 19).

(C) GABAergic mIPSCs in uninjured $Bax^{+/+}$ mice (n = 11) and $Bax^{+/+}$ mice 2 weeks after SNI (n = 14) and in uninjured $Bax^{-/-}$ mice (n = 8) and $Bax^{-/-}$ mice 2 weeks after SNI (n = 9).

*p < 0.05 and ***p < 0.001 in Student's t tests comparing uninjured $Bax^{+/+}$ mice and $Bax^{+/+}$ mice after SNI; $^{\#}p < 0.05$, $^{\#\#}p < 0.01$, and $^{\#\#\#}p < 0.001$ for the comparison between $Bax^{+/+}$ and $Bax^{-/-}$ mice after SNI. Error bars indicate SEM. See also Figure S5.

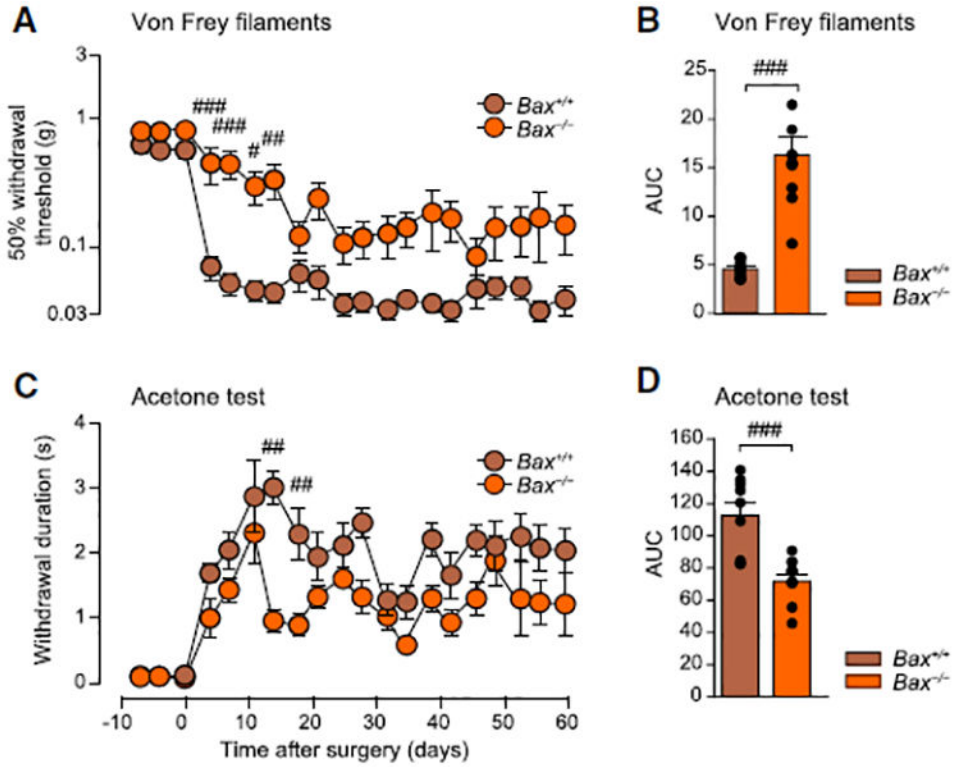

Figure 7. Disrupting the Intrinsic Apoptotic Pathway Reduces Neuropathic-Pain-like Behavior

(A and C) Withdrawal responses to (A) mechanical (von Frey filaments) or (C) cold stimulation (acetone evaporation) after SNI (n = 9). $p < 0.001$ for genotype and $p < 0.05$ for time when responses to the stimulation with von Frey filaments were compared in a two-way ANOVA. $p < 0.001$ for both genotype and time in the acetone test. Pound signs indicate the results of Bonferroni's tests following the ANOVAs.

(B and D) AUCs for the withdrawal responses to (B) mechanical or (D) cold stimulation were compared for the total test duration after SNI. Pound signs indicate the results of Student's t tests.

#$p < 0.05$, ##$p < 0.01$, and ###$p < 0.001$ in Student's t tests. Error bars indicate SEM.